Geometric measure of entanglement and applications to bipartite and multipartite quantum states

Tzu-Chieh Wei and Paul M. Goldbart
Department of Physics, University of Illinois at Urbana-Champaign, 1110 West Green Street, Urbana, Illinois 61801-3080, USA
(Received 25 March 2003; revised manuscript received 18 July 2003; published 9 October 2003)

The degree to which a pure quantum state is entangled can be characterized by the distance or angle to the nearest unentangled state. This geometric measure of entanglement, already present in a number of settings [A. Shimony, Ann. NY. Acad. Sci. **755**, 675 (1995); H. Barnum and N. Linden, J. Phys. A: Math. Gen. **34**, 6787 (2001)], is explored for bipartite and multipartite pure and mixed states. The measure is determined analytically for arbitrary two-qubit mixed states and for generalized Werner and isotropic states, and is also applied to certain multipartite mixed states. In particular, a detailed analysis is given for arbitrary mixtures of three-qubit Greenberger-Horne-Zeilinger, *W*, and inverted-*W* states. Along the way, we point out connections of the geometric measure of entanglement with entanglement witnesses and with the Hartree approximation method.

DOI: 10.1103/PhysRevA.68.042307 PACS number(s): 03.67.Mn, 03.65.Ud

I. INTRODUCTION

Only recently, after more than half a century of existence, has the notion of entanglement become recognized as central to quantum information processing [1]. As a result, the task of characterizing and quantifying entanglement has emerged as one of the prominent themes of quantum information theory. There have been many achievements in this direction, primarily in the setting of *bipartite* systems [2]. Among these, one highlight is Wootters' formula [3] for the entanglement of formation for two-qubit mixed states; others include corresponding results for highly symmetrical states of higher-dimensional systems [4,5]. The issue of entanglement for *multipartite* states poses an even greater challenge, and there have been correspondingly fewer achievements: notable examples include applications of the relative entropy [6], negativity [7], and Schmidt measure [8].

In this paper, we present an attempt to face this challenge by developing and investigating a certain geometric measure of entanglement (GME), first introduced by Shimony [9] in the setting of bipartite pure states and generalized to the multipartite setting (via projection operators of various ranks) by Barnum and Linden [10]. We begin by examining this geometric measure in pure-state settings and establishing a connection with entanglement witnesses and then extend the measure to mixed states, showing that it satisfies certain criteria required of good entanglement measures. We demonstrate that this geometric measure is no harder to compute than the entanglement of formation E_{F}, and exemplify this fact by giving formulas corresponding to E_{F} for (i) arbitrary two-qubit mixed, (ii) generalized Werner, and (iii) isotropic states. We conclude by applying the geometric entanglement measure to certain families of multipartite mixed states, for which we provide a practical method for computing entanglement and illustrate this method via several examples. In particular, a detailed analysis is given for arbitrary mixture of three-qubit Greenberger-Horne-Zeilinger (GHZ), *W*, and inverted-*W* states.

It is not our intention to cast aspersions on existing approaches to entanglement; rather we simply wish to add one further element to the discussion. Our discussion focuses on quantifying multipartite entanglement in terms of a single number rather than characterizing it.

The structure of the paper is as follows. In Sec. II we describe the basic geometric ideas on quantifying entanglement geometrically in the setting of pure quantum states and establish a connection with the Hartree approximation method and entanglement witnesses. In Sec. III we extend the definition of the GME to mixed states and show that it is an entanglement monotone. In Sec. IV we examine the GME for several families of mixed states of bipartite systems: (i) arbitrary two-qubit mixed, (ii) generalized Werner, (iii) isotropic states in bipartite systems, as well as (iv) certain mixtures of multipartite symmetric states. In Sec. V we give a detailed application of the GME to arbitrary mixtures of three-qubit GHZ, *W*, and inverted-*W* states. In Sec. VI we discuss some open questions and further directions. In the Appendix we briefly review the Vollbrecht-Werner technique used in the present paper.

II. BASIC GEOMETRIC IDEAS AND APPLICATION TO PURE STATES

We begin with an examination of entangled *pure* states and of how one might quantify their entanglement by making use of simple ideas of Hilbert space geometry. Let us start by developing a quite general formulation, appropriate for multipartite systems comprising n parts, in which each part can have a distinct Hilbert space. Consider a general n-partite pure state

$$|\psi\rangle = \sum_{p_1 \cdots p_n} \chi_{p_1 p_2 \cdots p_n} |e_{p_1}^{(1)} e_{p_2}^{(2)} \cdots e_{p_n}^{(n)}\rangle. \tag{1}$$

One can envisage a geometric definition of its entanglement content via the distance

$$d = \min_{|\phi\rangle} \| |\psi\rangle - |\phi\rangle \| \tag{2}$$

between $|\psi\rangle$ and the nearest separable state $|\phi\rangle$ (or equivalently the angle between them). Here, $|\phi\rangle \equiv \otimes_{i=1}^{n} |\phi^{(i)}\rangle$ is an arbitrary separable (i.e., Hartree) n-partite pure state, the index $i = 1, \ldots, n$ labels the parts, and

$$|\phi^{(i)}\rangle \equiv \sum_{p_i} c_{p_i}^{(i)} |e_{p_i}^{(i)}\rangle. \tag{3}$$

It seems natural to assert that the more entangled a state is, the further away it will be from its best unentangled approximant (and the wider will be the angle between them).

To actually find the nearest separable state, it is convenient to minimize, instead of d, the quantity

$$\| |\psi\rangle - |\phi\rangle \|^2, \tag{4}$$

subject to the constraint $\langle\phi|\phi\rangle = 1$. In fact, in solving the resulting stationarity condition one may restrict one's attention to the subset of solutions $|\phi\rangle$ that obey the further condition that for each factor $|\phi^{(i)}\rangle$ one has $\langle\phi^{(i)}|\phi^{(i)}\rangle = 1$. Thus, one arrives at the *nonlinear eigenproblem* for the stationary $|\phi\rangle$:

$$\sum_{p_1 \cdots \widehat{p_i} \cdots p_n} \chi^*_{p_1 p_2 \cdots p_n} c^{(1)*}_{p_1} \cdots \widehat{c^{(i)*}_{p_i}} \cdots c^{(n)*}_{p_n} = \Lambda\, c^{(i)*}_{p_i}, \tag{5a}$$

$$\sum_{p_1 \cdots \widehat{p_i} \cdots p_n} \chi_{p_1 p_2 \cdots p_n} c^{(1)*}_{p_1} \cdots \widehat{c^{(i)*}_{p_i}} \cdots c^{(n)*}_{p_n} = \Lambda\, c^{(i)*}_{p_i}, \tag{5b}$$

where the eigenvalue Λ is associated with the Lagrange multiplier enforcing the constraint $\langle\phi|\phi\rangle = 1$, and the symbol $\widehat{\ }$ denotes exclusion. In basis-independent form, Eqs. (5) read

$$\langle\psi| \left(\bigotimes_{j(\neq i)}^{n} |\phi^{(j)}\rangle \right) = \Lambda \langle\phi^{(i)}|, \tag{6a}$$

$$\left(\bigotimes_{j(\neq i)}^{n} \langle\phi^{(j)}| \right) |\psi\rangle = \Lambda |\phi^{(i)}\rangle. \tag{6b}$$

From Eqs. (5) or (6) one readily sees that the eigenvalues Λ are real, in $[-1,1]$, and independent of the choice of the local basis $\{|e_{p_i}^{(i)}\rangle\}$. Hence, the spectrum Λ is the cosine of the angle between $|\psi\rangle$ and $|\phi\rangle$; the largest, $\Lambda_{\max}$, which we call the *entanglement eigenvalue*, corresponds to the closest separable state and is equal to the maximal overlap

$$\Lambda_{\max} = \max_{\phi} |\langle\phi|\psi\rangle|, \tag{7}$$

where $|\phi\rangle$ is an arbitrary separable pure state.

Although, in determining the closest separable state, we have used the squared distance between the states, there are alternative (basis-independent) candidates for entanglement measures which are related to it in an elementary way: the distance, the sine, or the sine squared of the angle θ between them (with $\cos\theta \equiv \mathrm{Re}\langle\psi|\phi\rangle$). We shall adopt $E_{\sin^2} \equiv 1 - \Lambda_{\max}^2$ as our entanglement measure because, as we shall see, when generalizing $E_{\sin^2}$ to mixed states we have been able to show that it satisfies a set of criteria demanded of entanglement measures. We remark that determining the entanglement of $|\psi\rangle$ is equivalent to finding the Hartree approximation to the ground state of the auxiliary Hamiltonian $\mathcal{H} \equiv -|\psi\rangle\langle\psi|$ [11].

In bipartite applications, eigenproblem (5) is in fact *linear*, and solving it is actually equivalent to finding the Schmidt decomposition [9]. Moreover, the entanglement eigenvalue is equal to the maximal Schmidt coefficient. By contrast, for the case of three or more parts, the eigenproblem is a *nonlinear* one. As such, one can in general only address it directly, i.e., by determining the eigenvalues and eigenvectors simultaneously and numerically. Yet, as we shall illustrate shortly, there do exist certain families of pure states whose entanglement eigenvalues can be determined analytically.

A. Illustrative examples

Suppose we are already in possession of the Schmidt decomposition of some two-qubit pure state

$$|\psi\rangle = \sqrt{p}|00\rangle + \sqrt{1-p}|11\rangle. \tag{8}$$

Then we can read off the entanglement eigenvalue

$$\Lambda_{\max} = \max\{\sqrt{p}, \sqrt{1-p}\}. \tag{9}$$

Now, recall [3] that the concurrence C for this state is $2\sqrt{p(1-p)}$. Hence, one has

$$\Lambda_{\max}^2 = \tfrac{1}{2}(1 + \sqrt{1-C^2}), \tag{10}$$

which holds for arbitrary two-qubit pure states.

The possession of symmetry by a state can alleviate the difficulty associated with solving the nonlinear eigenproblem. To see this, consider a state

$$|\psi\rangle = \sum_{p_1 \cdots p_n} \chi_{p_1 p_2 \cdots p_n} |e_{p_1}^{(1)} e_{p_2}^{(2)} \cdots e_{p_n}^{(n)}\rangle \tag{11}$$

that obeys the symmetry that the nonzero amplitudes χ are invariant under permutations. What we mean by this is that, regardless of the dimensions of the factor Hilbert spaces, the amplitudes are only nonzero when the indices take on the first ν values (or can be arranged to do so by appropriate relabeling of the basis in each factor) and, moreover, that these amplitudes are invariant under permutations of the parties, i.e., $\chi_{\sigma_1 \sigma_2 \cdots \sigma_n} = \chi_{p_1 p_2 \cdots p_n}$, where the σ's are any permutation of the p's. (This symmetry may be obscured by arbitrary local unitary transformations.) For such states, it seems reasonable to anticipate that the closest Hartree approximant retains this permutation symmetry. Assuming this to be the case—and numerical experiments of ours support this assumption—in the task of determining the entanglement eigenvalue one can start with the ansatz that the closest separable state has the form

$$|\phi\rangle \equiv \bigotimes_{i=1}^{n} \left(\sum_j c_j |e_j^{(i)}\rangle \right), \tag{12}$$

i.e., is expressed in terms of copies of a single-factor state, for which $c_j^{(i)} = c_j$. To obtain the entanglement eigenvalue it is thus only necessary to maximize $\mathrm{Re}\langle\phi|\psi\rangle$ with respect to

$\{c_j\}_{j=1}^{\nu}$, a simpler task than maximization over the $\Sigma_{i=1}^{n} d_i$ amplitudes of a generic product state.

To illustrate this symmetry-induced simplification, we consider several examples involving permutation-invariant states, first restricting our attention to the case $\nu=2$. The most natural realizations are n-qubit systems. One can label these symmetric states according to the number of 0's, as follows [12]:

$$|S(n,k)\rangle \equiv \sqrt{\frac{k!(n-k)!}{n!}} \sum_{\text{permutations}} |\underbrace{0\cdots 0}_{k}\ \underbrace{1\cdots 1}_{n-k}\rangle. \tag{13}$$

As the amplitudes are all positive, one can assume that the closest Hartree state is of the form

$$|\phi\rangle = (\sqrt{p}|0\rangle + \sqrt{1-p}|1\rangle)^{\otimes n}, \tag{14}$$

for which the maximal overlap (with respect to p) gives the entanglement eigenvalue for $|S(n,k)\rangle$:

$$\Lambda_{\max}(n,k) = \sqrt{\frac{n!}{k!(n-k)!}} \left(\frac{k}{n}\right)^{k/2} \left(\frac{n-k}{n}\right)^{(n-k)/2}. \tag{15}$$

For fixed n, the minimum $\Lambda_{\max}$ (and hence the maximum entanglement) among the $|S(n,k)\rangle$'s occurs for $k=n/2$ (for n even) and $k=(n\pm 1)/2$ (for n odd). In fact, for fixed n the general permutation-invariant state can be expressed as $\Sigma_k \alpha_k |S(n,k)\rangle$ with $\Sigma_k |\alpha_k|^2 = 1$. The entanglement of such states can be addressed via the strategy that we have been discussing, i.e., via the maximization of a function of (at most) three real parameters. The simplest example is provided by the nGHZ state:

$$|n\text{GHZ}\rangle \equiv (|S(n,0)\rangle + |S(n,n)\rangle)/\sqrt{2}. \tag{16}$$

It is easy to show that (for all n) $\Lambda_{\max}(n\text{GHZ}) = 1/\sqrt{2}$ and $E_{\sin^2} = 1/2$.

We now focus our attention on three-qubit settings. Of these, the states $|S(3,0)\rangle = |000\rangle$ and $|S(3,3)\rangle = |111\rangle$ are not entangled and are, respectively, the components of the 3-GHZ state: $|\text{GHZ}\rangle \equiv (|000\rangle + |111\rangle)/\sqrt{2}$. The states $|S(3,2)\rangle$ and $|S(3,1)\rangle$, denoted as

$$|W\rangle \equiv |S(3,2)\rangle = (|001\rangle + |010\rangle + |100\rangle)/\sqrt{3}, \tag{17a}$$

$$|\widetilde{W}\rangle \equiv |S(3,1)\rangle = (|110\rangle + |101\rangle + |011\rangle)/\sqrt{3}, \tag{17b}$$

are equally entangled, having $\Lambda_{\max} = 2/3$ and $E_{\sin^2} = 5/9$.

Next, consider a superposition of the W and $\widetilde{W}$ states:

$$|W\widetilde{W}(s,\phi)\rangle \equiv \sqrt{s}|W\rangle + \sqrt{1-s}e^{i\phi}|\widetilde{W}\rangle. \tag{18}$$

It is easy to see that its entanglement is independent of ϕ: the transformation $\{|0\rangle,|1\rangle\} \to \{|0\rangle, e^{-i\phi}|1\rangle\}$ induces $|W\widetilde{W}(s,\phi)\rangle \to e^{-i\phi}|W\widetilde{W}(s,0)\rangle$. To calculate $\Lambda_{\max}$, we assume that the separable state is $(\cos\theta|0\rangle + \sin\theta|1\rangle)^{\otimes 3}$ and maximize its overlap with $|W\widetilde{W}(s,0)\rangle$. Thus we find that the tangent $t \equiv \tan\theta$ is the particular root of the polynomial equation

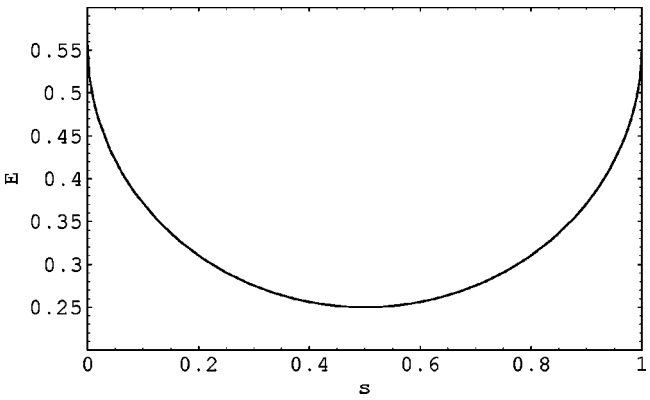

FIG. 1. Entanglement of the pure state $\sqrt{s}|W\rangle + \sqrt{1-s}|\widetilde{W}\rangle$ vs s. This also turns out to be the entanglement curve for the mixed state $s|W\rangle\langle W| + (1-s)|\widetilde{W}\rangle\langle\widetilde{W}|$.

$$\sqrt{1-s}t^3 + 2\sqrt{s}t^2 - 2\sqrt{1-s}t - \sqrt{s} = 0 \tag{19}$$

that lies in the range $t \in [\sqrt{1/2}, \sqrt{2}]$. Via $\theta(s)$, $\Lambda_{\max}$ (and thus $E_{\sin^2} = 1 - \Lambda_{\max}^2$) can be expressed as

$$\Lambda_{\max}(s) = \tfrac{1}{2}[\sqrt{s}\cos\theta(s) + \sqrt{1-s}\sin\theta(s)]\sin 2\theta(s). \tag{20}$$

In Fig. 1, we show $E_{\sin^2}(|W\widetilde{W}(s,\phi)\rangle)$ vs s. In fact, $\Lambda_{\max}$ for the more general superposition

$$|SS_{n;k_1k_2}(r,\phi)\rangle \equiv \sqrt{r}|S(n,k_1)\rangle + \sqrt{1-r}e^{i\phi}|S(n,k_2)\rangle \tag{21}$$

(with $k_1 \neq k_2$) turns out to be independent of ϕ, as in the case of $|W\widetilde{W}(s,\phi)\rangle$, and can be computed in the same way. We note that although the curve in Fig. 1 is convex, convexity does not hold uniformly over k_1 and k_2.

As our last pure-state example in the qubit setting, we consider superpositions of W and GHZ states:

$$|\Psi_{\text{GHZ+W}}(s,\phi)\rangle \equiv \sqrt{s}|\text{GHZ}\rangle + \sqrt{1-s}e^{i\phi}|W\rangle. \tag{22}$$

For these, the phase ϕ cannot be "gauged" away and, hence, $E_{\sin^2}$ depends on ϕ.

In Fig. 2 we show $E_{\sin^2}$ vs s at $\phi=0$ and $\phi=\pi$ (i.e., the bounding curves), as well as $E_{\sin^2}$ for randomly generated values of $s \in [0,1]$ and $\phi \in [0,2\pi]$ (dots). It is interesting to observe that the "π" state has higher entanglement than the "0" does. As the numerical results suggest, the (ϕ parametrized) $E_{\sin^2}$ vs s curves of the states $|\Psi_{\text{GHZ+W}}(s,\phi)\rangle$ lie between the π and 0 curves.

We remark that, more generally, systems comprising n parts, each a d-level system, the symmetric state

$$|S(n;\{k\})\rangle \equiv \sqrt{\frac{\Pi_i k_i!}{n!}} \sum_{\text{P}} |\underbrace{0..0}_{k_0}\ \underbrace{1..1}_{k_1} \ldots \underbrace{(d-1)\ldots(d-1)}_{k_{d-1}}\rangle, \tag{23}$$

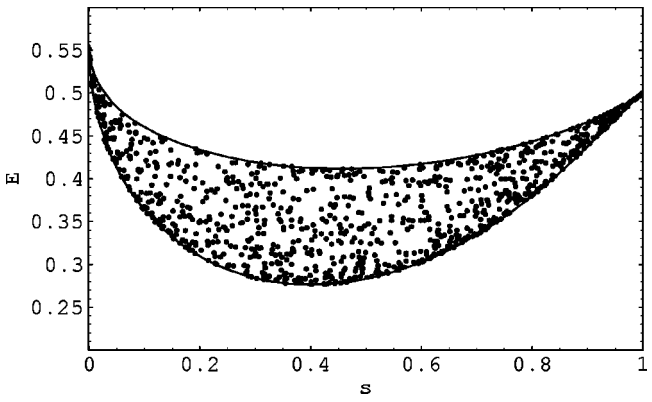

FIG. 2. Entanglement of $|\Psi_{\mathrm{GHZ+W}}(s,\phi)\rangle$ vs s. The upper curve is for $\phi=\pi$ whereas the lower one is for $\phi=0$. Dots represent states with randomly generated s and ϕ.

with $\Sigma_i k_i = n$, has entanglement eigenvalue

$$\Lambda_{\max}(n;\{k\}) = \sqrt{\frac{n!}{\Pi_i(k_i!)}} \prod_{i=0}^{d-1} \left(\frac{k_i}{n}\right)^{k_i/2}. \tag{24}$$

One can also consider other symmetries. For example, for the totally antisymmetric (viz., determinant) state of n parts, each with n levels,

$$|\mathrm{Det}_n\rangle \equiv \frac{1}{\sqrt{n!}} \sum_{i_1,\ldots,i_n=1}^{n} \epsilon_{i_1,\ldots,i_n} |i_1,\ldots,i_n\rangle, \tag{25}$$

it has been shown by Bravyi [13] that the maximal squared overlap is $\Lambda^2_{\max}=1/n!$. Bravyi also generalized the antisymmetric state to the $n=pd^p$-partite determinant state via

$$\phi(1)=(0,0,\ldots,0,0),$$

$$\phi(2)=(0,0,\ldots,0,1),$$

$$\vdots$$

$$\phi(d^p-1)=(d-1,d-1,\ldots,d-1,d-2),$$

$$\phi(d^p)=(d-1,d-1,\ldots,d-1,d-1),$$

and

$$|\mathrm{Det}_{n,d}\rangle \equiv \frac{1}{\sqrt{(d^p!)}} \sum_{i_1,\ldots,i_{d^p}} \epsilon_{i_1,\ldots,i_{d^p}} |\phi(i_1),\ldots,\phi(i_{d^p})\rangle. \tag{26}$$

In this case, one can show that $\Lambda^2_{\max}=[(d^p)!]^{-1}$.

B. Connection with entanglement witnesses

We now digress to discuss the relationship between the geometric measure of entanglement and another entanglement property—entanglement witnesses. The entanglement witness $\mathcal{W}$ for an entangled state ρ is defined to be an operator that is (a) Hermitian and (b) obeys the following conditions [14]: (i) $\mathrm{Tr}(\mathcal{W}\sigma)\geqslant 0$ for all separable states σ and (ii) $\mathrm{Tr}(\mathcal{W}\rho)<0$. Here, we wish to establish a correspondence between $\Lambda_{\max}$ for the entangled pure state $|\psi\rangle$ and the optimal element of the set of entanglement witnesses $\mathcal{W}$ for $|\psi\rangle$ that have the specific form

$$\mathcal{W}=\lambda^2\mathbb{1}-|\psi\rangle\langle\psi|, \tag{27}$$

this set being parametrized by the real, non-negative number λ^2. By *optimal* we mean that, for this specific form of witnesses, the value of the " detector" $\mathrm{Tr}(\mathcal{W}|\psi\rangle\langle\psi|)$ is as negative as can be.

In order to satisfy condition (i) we must ensure that, for any *separable* state σ, we have $\mathrm{Tr}(\mathcal{W}\sigma)\geqslant 0$. As the density matrix for any separable state can be decomposed into a mixture of *separable pure* states [i.e., $\sigma=\Sigma_i|\phi_i\rangle\langle\phi_i|$, where $\{|\phi_i\rangle\}$ are separable pure states], condition (i) will be satisfied as long as $\mathrm{Tr}(\mathcal{W}|\phi\rangle\langle\phi|)\geqslant 0$ for all separable *pure* states $|\phi\rangle$. This condition is equivalent to

$$\lambda^2-||\langle\psi|\phi\rangle||^2\geqslant 0 \quad \text{for all separable } |\phi\rangle, \tag{28}$$

which leads to

$$\lambda^2\geqslant \max_{|\phi\rangle}||\langle\psi|\phi\rangle||^2=\Lambda^2_{\max}(|\psi\rangle). \tag{29}$$

Condition (ii) requires that $\mathrm{Tr}(\mathcal{W}|\psi\rangle\langle\psi|)<0$, in order for $\mathcal{W}$ to be a valid entanglement witness for $|\psi\rangle$; this gives $\lambda^2-1<0$. Thus, we have established the range of λ for which $\lambda^2\mathbb{1}-|\psi\rangle\langle\psi|$ is a valid entanglement witness for $|\psi\rangle$:

$$\Lambda^2_{\max}(|\psi\rangle)\leqslant\lambda^2<1. \tag{30}$$

With these preliminaries in place, we can now establish the connection we are seeking. Of the specific family (27) of entanglement witnesses for $|\psi\rangle$, the one of the form $\mathcal{W}_{\mathrm{opt}}=\Lambda^2_{\max}(|\psi\rangle)\mathbb{1}-|\psi\rangle\langle\psi|$ is optimal, in the sense that it achieves the most negative value for the detector $\mathrm{Tr}(\mathcal{W}_{\mathrm{opt}}|\psi\rangle\langle\psi|)$:

$$\min_{\mathcal{W}}\mathrm{Tr}(\mathcal{W}|\psi\rangle\langle\psi|)=\mathrm{Tr}(\mathcal{W}_{\mathrm{opt}}|\psi\rangle\langle\psi|)=-E_{\sin^2}(|\psi\rangle), \tag{31}$$

where $\mathcal{W}$ runs over class (27) of witnesses.

We now look at some examples. For the GHZ state the optimal witness is

$$\mathcal{W}_{\mathrm{GHZ}}=\tfrac{1}{2}\mathbb{1}-|\mathrm{GHZ}\rangle\langle\mathrm{GHZ}| \tag{32}$$

and $\mathrm{Tr}(\mathcal{W}_{\mathrm{GHZ}}|\mathrm{GHZ}\rangle\langle\mathrm{GHZ}|)=-E_{\sin^2}(|\mathrm{GHZ}\rangle)=-1/2$. Similarly, for the W and inverted-W states we have

$$\mathcal{W}_W=\tfrac{4}{9}\mathbb{1}-|W\rangle\langle W| \quad \text{and} \quad \mathcal{W}_{\tilde{W}}=\tfrac{4}{9}\mathbb{1}-|\tilde{W}\rangle\langle\tilde{W}| \tag{33}$$

and $\mathrm{Tr}(\mathcal{W}_W|W\rangle\langle W|)=-E_{\sin^2}(|W\rangle)=-5/9$, and similarly for $|\tilde{W}\rangle$. For the four-qubit state

$$|\Psi\rangle\equiv(|0011\rangle+|0101\rangle+|0110\rangle+|1001\rangle+|1010\rangle+|1100\rangle)/\sqrt{6}, \tag{34}$$

the optimal witness is

$$\mathcal{W}_\Psi = \tfrac{3}{8}\mathbb{1} - |\Psi\rangle\langle\Psi| \tag{35}$$

and $\mathrm{Tr}(\mathcal{W}_\Psi|\Psi\rangle\langle\Psi|) = -E_{\sin^2}(|\Psi\rangle) = -5/8$.

Although the observations we have made in this section are, from a technical standpoint, elementary, we nevertheless find it intriguing that two distinct aspects of entanglement—the geometric measure of entanglement and entanglement witnesses—are so closely related. Furthermore, this connection sheds light on the content of the geometric measure of entanglement. In particular, as entanglement witnesses are Hermitian operators, they can, at least in principle, be realized and measured locally [15]. Their connection with the geometric measure of entanglement ensures that the geometric measure of entanglement can, at least in principle, be verified experimentally.

III. EXTENSION TO MIXED STATES

The extension of the GME to mixed states ρ can be made via the use of the *convex roof* (or *hull*) construction [indicated by $\mathcal{C}_{\mathrm{conv}}$], as was done for the entanglement of formation (see, e.g., Ref. [3]). The essence is a minimization over all decompositions $\rho = \Sigma_i p_i |\psi_i\rangle\langle\psi_i|$ into pure states, i.e.,

$$E(\rho) \equiv \mathcal{C}_{\mathrm{conv}} E_{\mathrm{pure}}(\rho) \equiv \min_{\{p_i,\psi_i\}} \sum_i p_i E_{\mathrm{pure}}(|\psi_i\rangle). \tag{36}$$

Now, any good entanglement measure E should, at least, satisfy the following criteria (cf. Refs. [6,16,17]): (C1) (a) $E(\rho) \geqslant 0$, (b) $E(\rho) = 0$ if ρ is not entangled; (C2) local unitary transformations do not change E; (C3) local operations and classical communication (LOCC) (as well as postselection) do not increase the expectation value of E; and (C4) entanglement is convex under the discarding of information, i.e., $\Sigma_i p_i E(\rho_i) \geqslant E(\Sigma_i p_i \rho_i)$.

The issue of the desirability of additional features, such as continuity and additivity, requires further investigation, but criteria (C1)–(C4) are regarded as the minimal set, if one is to guarantee that one has an *entanglement monotone* [17].

Does the geometric measure of entanglement obey criteria (C1)–(C4)? From definition (36) it is evident that criteria (C1) and (C2) are satisfied, provided that E_{pure} satisfies them, as it does for E_{pure} being any function of $\Lambda_{\max}$ consistent with criterion (C1). It is straightforward to check that criterion (C4) holds by the convex-hull construction. The consideration of criterion (C3) seems to be more delicate. The reason is that our analysis of whether or not it holds depends on the explicit form of E_{pure}. For criterion (C3) to hold, it is sufficient to show that the average entanglement is nonincreasing under any trace-preserving, unilocal operation: $\rho \to \Sigma_k V_k \rho V_k^\dagger$, where the Kraus operator has the form $V_k = \mathbb{1} \otimes \cdots \mathbb{1} \otimes V_k^{(i)} \otimes \mathbb{1} \cdots \otimes \mathbb{1}$ and $\Sigma_k V_k^\dagger V_k = \mathbb{1}$. Furthermore, it suffices to show that criterion (C3) holds for the case of a pure initial state, i.e., $\rho = |\psi\rangle\langle\psi|$.

We now prove that for the particular (and by no means unnatural) choice $E_{\mathrm{pure}} = E_{\sin^2}$, criterion (C3) holds. To be precise, for any quantum operation on a pure initial state, i.e.,

$$|\psi\rangle\langle\psi| \to \sum_k V_k |\psi\rangle\langle\psi| V_k^\dagger, \tag{37}$$

we aim to show that

$$\sum_k p_k E_{\sin^2}(V_k|\psi\rangle/\sqrt{p_k}) \leqslant E_{\sin^2}(|\psi\rangle), \tag{38}$$

where $p_k \equiv \mathrm{Tr}\, V_k|\psi\rangle\langle\psi|V_k^\dagger = \langle\psi|V_k^\dagger V_k|\psi\rangle$, regardless of whether the operation $\{V_k\}$ is state to state or state to ensemble. Let us, respectively, denote by Λ and Λ_k the entanglement eigenvalues corresponding to $|\psi\rangle$ and the (normalized) pure state $V_k|\psi\rangle/\sqrt{p_k}$. Then our task is to show that $\Sigma_k p_k \Lambda_k^2 \geqslant \Lambda^2$, of which the left-hand side is, by the definition of Λ_k, equivalent to

$$\sum_k p_k \max_{\xi_k \in D_s} \|\langle\xi_k|V_k|\psi\rangle/\sqrt{p_k}\|^2 = \sum_k \max_{\xi_k \in D_s} \|\langle\xi_k|V_k|\psi\rangle\|^2. \tag{39}$$

Without loss of generality, we may assume that it is the first party that performs the operation. Recall that condition (6) for the closest separable state

$$|\phi\rangle \equiv |\tilde{\alpha}\rangle_1 \otimes |\tilde{\gamma}\rangle_{2\cdots n} \tag{40}$$

can be recast as

$${}_{2\cdots n}\langle\tilde{\gamma}|\psi\rangle_{1\cdots n} = \Lambda|\tilde{\alpha}\rangle_1. \tag{41}$$

Then, by making the specific choice

$$\langle\xi_k| = (\langle\tilde{\alpha}|V_k^{(1)\dagger}/\sqrt{q_k}) \otimes \langle\tilde{\gamma}|, \tag{42}$$

where $q_k \equiv \langle\tilde{\alpha}|V_k^{(1)\dagger}V_k^{(1)}|\tilde{\alpha}\rangle$, we have the sought result

$$\sum_k p_k \Lambda_k^2 = \sum_k \max_{\xi_k \in D_s} \|\langle\xi_k|V_k|\psi\rangle\|^2 \geqslant \Lambda^2 \sum_k (\langle\tilde{\alpha}|V_k^{(1)\dagger}V_k^{(1)}|\tilde{\alpha}\rangle/\sqrt{q_k})^2 = \Lambda^2. \tag{43}$$

Hence, the form $1-\Lambda^2$, when generalized to mixed states, is an entanglement monotone. We note that a different approach to establishing this result has been used by Barnum and Linden [10]. Moreover, using the result that $\Sigma_k p_k \Lambda_k^2 \geqslant \Lambda^2$, one can further show that for any convex increasing function $f_c(x)$ with $x \in [0,1]$,

$$\sum_k p_k f_c(\Lambda_k^2) \geqslant f_c(\Lambda^2). \tag{44}$$

Therefore, the quantity $\mathrm{const} - f_c(\Lambda^2)$ (where the const is to ensure the whole expression is non-negative), when extended to mixed states, is also an entanglement monotone, hence a good entanglement measure. For the following discussion we simply take $E = 1 - \Lambda^2$.

IV. ANALYTIC RESULTS FOR MIXED STATES

Before moving on to the *terra incognita* of mixed *multipartite* entanglement, we test the geometric approach in the setting of mixed *bipartite* states by computing $E_{\sin^2}$ for three classes of states for which E_{F} is known.

A. Arbitrary two-qubit mixed states

For these we show that

$$E_{\sin^2}(\rho)=\tfrac{1}{2}[1-\sqrt{1-C(\rho)^2}], \tag{45}$$

where $C(\rho)$ is the Wootters concurrence of the state ρ. Recall that in his derivation of the formula for E_{F}, Wootters showed that there exists an optimal decomposition $\rho=\Sigma_i p_i|\psi_i\rangle\langle\psi_i|$ in which every $|\psi_i\rangle$ has the concurrence of ρ itself. (More explicitly, every $|\psi_i\rangle$ has the identical concurrence, the concurrence being the infimum over all decompositions.) By using Eq. (10) one can, via Eq. (45), relate $E_{\sin^2}$ to C for any two-qubit *pure* state. As $E_{\sin^2}$ is a monotonically increasing convex function of $C\in[0,1]$, the optimal decomposition for $E_{\sin^2}$ is identical to that for the entanglement of formation E_{F}. Thus, we see that Eq. (45) holds for *any two-qubit mixed state*.

The fact that $E_{\sin^2}$ is related to E_{F} via the concurrence C is inevitable for two-qubit systems, as both are fully determined by the one independent Schmidt coefficient. We note that Vidal [18] had derived this expression when he had considered the probability of success for converting a single copy of some pure state into the desired mixed state, which gives a physical interpretation of the geometric measure of entanglement. Unfortunately, this connection only holds for two-qubit states.

B. Generalized Werner states

Any state ρ_W of a $C^d\otimes C^d$ system is called a generalized Werner state if it is invariant under

$$\mathbf{P}_1:\rho\rightarrow\int dU(U\otimes U)\rho(U^\dagger\otimes U^\dagger), \tag{46}$$

where U is any element of the unitary group $\mathcal{U}(d)$ and dU is the corresponding normalized Haar measure. Such states can be expressed as a linear combination of two operators: the *identity* $\hat{\mathbb{1}}$ and the *swap* $\hat{F}\equiv\Sigma_{ij}|ij\rangle\langle ji|$, i.e., $\rho_W\equiv a\hat{\mathbb{1}}+b\hat{F}$, where a and b are real parameters related via the constraint $\mathrm{Tr}\,\rho_W=1$. This one-parameter family of states can be neatly expressed in terms of the single parameter $f\equiv\mathrm{Tr}(\rho_W\hat{F})$:

$$\rho_W(f)=\frac{d^2-fd}{d^4-d^2}\mathbb{1}\otimes\mathbb{1}+\frac{fd^2-d}{d^4-d^2}\hat{F}. \tag{47}$$

By applying to $E_{\sin^2}$ the technique developed by Vollbrecht and Werner for $E_{\mathrm{F}}(\rho_W)$ (see Ref. [4] or Appendix A), one arrives at the geometric entanglement function for Werner states:

$$E_{\sin^2}(\rho_W(f))=\frac{1}{2}(1-\sqrt{1-f^2}) \quad \text{for} \quad f\leqslant 0, \tag{48}$$

and 0 otherwise.

The essential points of the derivation are as follows. (i) In order to find the set M_{ρ_W} (see Appendix A) it is sufficient, due to the invariance of ρ_W under $\mathbf{P_1}$, to consider any pure state $|\Phi\rangle=\Sigma_{jk}\Phi_{jk}|e_j^{(1)}\rangle\otimes|e_k^{(2)}\rangle$ that has a diagonal reduced density matrix $\mathrm{Tr}_2|\Phi\rangle\langle\Phi|$ and the value $\mathrm{Tr}(|\Phi\rangle\langle\Phi|\hat{F})$ equal to the parameter f associated with the Werner state $\rho_W(f)$. It can be shown that

$$E_{\sin^2}(|\Phi\rangle\langle\Phi|)\geqslant\frac{1}{2}\left[1-\sqrt{1-\left(f-\sum_i\lambda_{ii}\right)^2}\right], \tag{49}$$

where $\lambda_{ii}\equiv|\Phi_{ii}|^2$.

(ii) If $f>0$, we can set the only nonzero elements of $|\Phi\rangle$ to be Φ_{i1}, Φ_{i2}, ..., Φ_{ii}, ..., Φ_{id} such that $|\Phi_{ii}|^2=f$, this state obviously being separable. Hence, for $f>0$ we have $E_{\sin^2}(\rho_W(f))=0$. On the other hand, if $f<0$, then any nonzero λ_{ii} would increase $(f-\Sigma_i\lambda_{ii})^2$ and, hence, increase the value of $E(|\Phi\rangle\langle\Phi|)$, not conforming with the convex hull. Thus, for a fixed value of f, the lowest possible value of the entanglement $E(|\Phi\rangle\langle\Phi|)$ that can be achieved occurs when $\lambda_{ii}=0$ and there are only two nonzero elements Φ_{ij} and Φ_{ji} $(i\neq j)$. This leads to

$$\min_{|\Phi\rangle\text{ at fixed }f}E(|\Phi\rangle\langle\Phi|)=\frac{1}{2}(1-\sqrt{1-f^2}). \tag{50}$$

Thus, as a function of f, $\epsilon(f)$ is given by

$$\epsilon(f)=\begin{cases}\dfrac{1}{2}(1-\sqrt{1-f^2}) & \text{for } f\leqslant 0,\\ 0 & \text{for } f\geqslant 0,\end{cases} \tag{51}$$

which, being convex for $f\in[-1,1]$, gives the entanglement function (48) for Werner states.

C. Isotropic states

These are states invariant under

$$\mathbf{P}_2:\rho\rightarrow\int dU(U\otimes U^*)\rho(U^\dagger\otimes U^{*\dagger}), \tag{52}$$

and can be expressed as

$$\rho_{\mathrm{iso}}(F)\equiv\frac{1-F}{d^2-1}(\hat{\mathbb{1}}-|\Phi^+\rangle\langle\Phi^+|)+F|\Phi^+\rangle\langle\Phi^+|, \tag{53}$$

where $|\Phi^+\rangle\equiv 1/\sqrt{d}\,\Sigma_{i=1}^d|ii\rangle$ and $F\in[0,1]$. For $F\in[0,1/d]$ this state is known to be separable [19]. By following arguments similar to those applied by Terhal and Vollbrecht [5] for $E_{\mathrm{F}}(\rho_{\mathrm{iso}})$ one arrives at

$$E_{\sin^2}(\rho_{\mathrm{iso}}(F))=1-\frac{1}{d}(\sqrt{F}+\sqrt{(1-F)(d-1)})^2, \tag{54}$$

for $F \geqslant 1/d$. The essential point of the derivation is the following Lemma (cf. Ref. [5]).

Lemma. The entanglement $E_{\sin^2}$ for isotropic states in $C^d \otimes C^d$ for $F \in [1/d,1]$ is given by

$$E_{\sin^2}(\rho_{\mathrm{iso}}(F)) = \mathcal{C}_{\mathrm{conv}}(R(F)), \tag{55}$$

where $\mathcal{C}_{\mathrm{conv}}(R(F))$ is the convex hull of the function R and

$$R(F) = 1 - \max_{\{\mu_i\}} \left\{ \mu_i \middle| F = \left(\sum_{i=1}^{d} \sqrt{\mu_i} \right)^2 \Big/ d; \quad \sum_{i=1}^{d} \mu_i = 1 \right\}. \tag{56}$$

Straightforward extremization shows that

$$R(F) = 1 - \left(\sqrt{\frac{F}{d}} + \sqrt{\frac{F+d-1}{d} - F} \right)^2, \tag{57}$$

which is convex, and hence $\mathcal{C}_{\mathrm{conv}}(R(F)) = R(F)$. Thus we arrive at the entanglement result for isotropic states given in Eq. (54).

D. Mixtures of multipartite symmetric states

Before exploring more general mixed states, it is useful to first examine states with high symmetry. With this in mind, we consider states formed by mixing two distinct symmetric states (i.e., $k_1 \neq k_2$):

$$\rho_{n;k_1k_2}(r) \equiv r|S(n,k_1)\rangle\langle S(n,k_1)| + (1-r)|S(n,k_2)\rangle \times \langle S(n,k_2)|. \tag{58}$$

From the independence of $E_{\sin^2}(|SS_{n;k_1k_2}(r,\phi)\rangle)$ on ϕ and the fact that the mixed state $\rho_{n;k_1k_2}(r)$ is invariant under the projection

$$\mathbf{P}_3 : \rho \rightarrow \int \frac{d\phi}{2\pi} U^{\otimes n} \rho U^{\dagger \otimes n} \tag{59}$$

with $U: \{|0\rangle, |1\rangle\} \rightarrow \{|0\rangle, e^{-i\phi}|1\rangle\}$, we have that $E_{\sin^2}(\rho_{n;k_1k_2}(r))$ vs r can be constructed from the convex hull of the entanglement function of $|SS_{n;k_1k_2}(r,0)\rangle$ vs r. An example, $(n,k_1,k_2) = (7,2,5)$, is shown in Fig. 3. If the dependence of $E_{\sin^2}$ on r is already convex for the pure state, its mixed-state counterpart has precisely the same dependence. Figure 1, for which $(n,k_1,k_2) = (3,1,2)$, exemplifies such behavior. More generally, one can consider mixed states of the form

$$\rho(\{p\}) = \sum_k p_k |S(n,k)\rangle\langle S(n,k)|. \tag{60}$$

The entanglement $E_{\mathrm{mixed}}(\{p\})$ can then be obtained as a function of the mixture $\{p\}$ from the convex hull of the entanglement function $E_{\mathrm{pure}}(\{q\})$ for the *pure* state $\Sigma_k \sqrt{q_k}|S(n,k)\rangle$. That is, $E_{\mathrm{mix}}(\{p\}) = \mathcal{C}_{\mathrm{conv}} E_{\mathrm{pure}}(\{q\} = \{p\})$. Therefore, the entanglement for a mixture of symmetric states $|S(n,k)\rangle$ is known, up to some convexification.

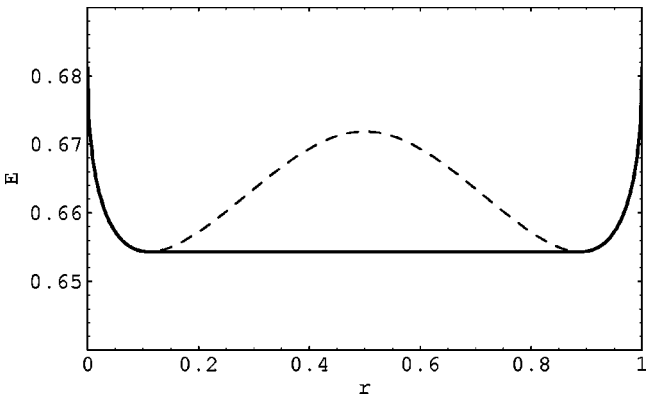

FIG. 3. Entanglement curve for the mixed state $\rho_{7;2,5}(r)$ (full line) constructed as the convex hull of the curve for the pure state $|SS_{7;2,5}(r,\phi)\rangle$ (dashed in the middle; full at the edges).

V. APPLICATION TO ARBITRARY MIXTURE OF GHZ, *W*, AND INVERTED-*W* STATES

Having warmed up in Sec. IV D by analyzing mixtures of multipartite symmetric states, we now turn our attention to mixtures of three-qubit GHZ, *W*, and inverted-*W* states.

A. Symmetry and entanglement preliminaries

These states are important, in the sense that all pure states can, under stochastic LOCC, be transformed either to GHZ or *W* (equivalently inverted-*W*) states. It is thus interesting to determine the entanglement content (using any measure of entanglement) for mixed states of the form

$$\rho(x,y) \equiv x|\mathrm{GHZ}\rangle\langle\mathrm{GHZ}| + y|W\rangle\langle W| + (1-x-y)|\tilde{W}\rangle\langle\tilde{W}|, \tag{61}$$

where $x,y \geqslant 0$ and $x+y \leqslant 1$. This family of mixed states is not contained in family (60), as $|\mathrm{GHZ}\rangle = (|S(3,0)\rangle + |S(3,3)\rangle)/\sqrt{2}$. The property of $\rho(x,y)$ that facilitates the computation of its entanglement is a certain invariance, which we now describe. Consider the local unitary transformation on a single qubit:

$$|0\rangle \rightarrow |0\rangle, \tag{62a}$$

$$|1\rangle \rightarrow g^k|1\rangle, \tag{62b}$$

where $g = \exp(2\pi i/3)$, i.e., a relative phase shift. This transformation, when applied simultaneously to all three qubits, is denoted by U_k. It is straightforward to see that $\rho(x,y)$ is invariant under the mapping

$$\mathbf{P}_4 : \rho \rightarrow \frac{1}{3} \sum_{k=1}^{3} U_k \rho U_k^{\dagger}. \tag{63}$$

Thus, we can apply Vollbrecht-Werner technique [4] to the computation of the entanglement of $\rho(x,y)$.

Now, the Vollbrecht-Werner procedure requires one to characterize the set S_{inv} of all pure states that are invariant under the projection $\mathbf{P}_4$. Then, the convex hull of $E_{\sin^2}(\rho)$ need only be taken over S_{inv}, instead of the set of *all* pure

states. However, as the state $\rho(x,y)$ is a mixture of three orthogonal pure states ($|\mathrm{GHZ}\rangle$, $|W\rangle$, and $|\widetilde{W}\rangle$) that are themselves invariant under $\mathbf{P}_4$, the pure states that can enter any possible decomposition of ρ must be of the restricted form

$$\alpha|\mathrm{GHZ}\rangle+\beta|W\rangle+\gamma|\widetilde{W}\rangle, \tag{64}$$

with $|\alpha|^2+|\beta|^2+|\gamma|^2=1$. Thus, there is no need to characterize S_{inv}, but rather to characterize the pure states that, under $\mathbf{P}_4$, are projected to $\rho(x,y)$. These states are readily seen to be of the form

$$\sqrt{x}e^{i\phi_1}|\mathrm{GHZ}\rangle+\sqrt{y}e^{i\phi_2}|W\rangle+\sqrt{1-x-y}e^{i\phi_3}|\widetilde{W}\rangle. \tag{65}$$

Of these, the least entangled state, for (x,y) given, has all coefficients non-negative (up to a global phase), i.e.,

$$|\psi(x,y)\rangle\equiv\sqrt{x}|\mathrm{GHZ}\rangle+\sqrt{y}|W\rangle+\sqrt{1-x-y}|\widetilde{W}\rangle. \tag{66}$$

The entanglement eigenvalue of $|\psi(x,y)\rangle$ can then be readily calculated, and one obtains

$$\Lambda(x,y)=\frac{1}{(1+t^2)^{3/2}}\left\{\sqrt{\frac{x}{2}}(1+t^3)+\sqrt{3y}t+\sqrt{3(1-x-y)}t^2\right\}, \tag{67}$$

where t is the (unique) non-negative real root of the following third-order polynomial equation:

$$3\sqrt{\frac{x}{2}}(-t+t^2)+\sqrt{3y}(-2t^2+1)+\sqrt{3(1-x-y)}\times(-t^3+2t)=0. \tag{68}$$

Hence, the entanglement function for $|\psi(x,y)\rangle$, i.e., $E_\psi(x,y)\equiv 1-\Lambda(x,y)^2$, is determined (up to the straightforward task of root finding).

B. Finding the convex hull

Recall that our aim is to determine the entanglement of the mixed state $\rho(x,y)$. As we already know the entanglement of the corresponding pure state $|\psi(x,y)\rangle$, we may accomplish our aim by the Vollbrecht-Werner technique [4], which gives the entanglement of $\rho(x,y)$ in terms of that of $|\psi(x,y)\rangle$ via the convex-hull construction: $E_\rho(x,y)=\mathcal{C}_{\mathrm{conv}}E_\psi(x,y)$. Put in words, the entanglement surface $z=E_\rho(x,y)$ is the convex surface constructed from the surface $z=E_\psi(x,y)$.

The idea underlying the use of the convex hull is this. Due to its linearity in x and y, state $\rho(x,y)$ (61) can [except when (x,y) lies on the boundary] be decomposed into two parts:

$$\rho(x,y)=p\rho(x_1,y_1)+(1-p)\rho(x_2,y_2), \tag{69}$$

with the weight p and end points (x_1,y_1) and (x_2,y_2) related by

$$px_1+(1-p)x_2=x, \tag{70a}$$

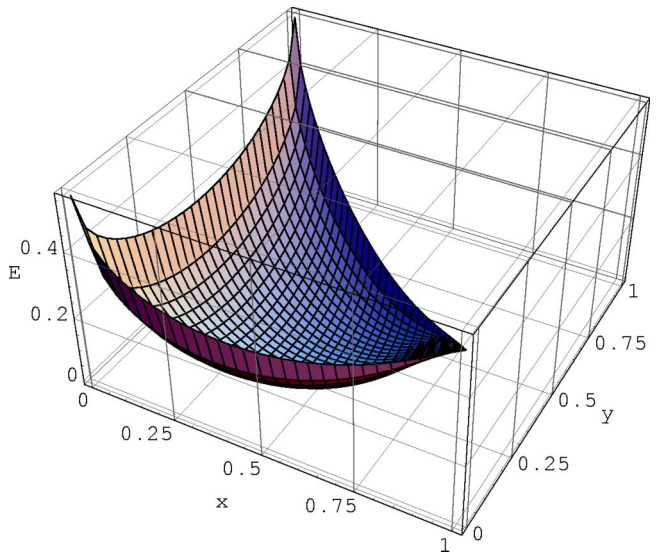

FIG. 4. (Color online) Entanglement vs the composition of the pure state $|\psi(x,y)\rangle$. This entanglement surface is not convex near $(x,y)=(1,0)$, although not obvious from the plot.

$$py_1+(1-p)y_2=y. \tag{70b}$$

Now, if it should happen that

$$pE_\psi(x_1,y_1)+(1-p)E_\psi(x_2,y_2)<E_\psi(x,y), \tag{71}$$

then the entanglement, averaged over the end points, would give a value lower than that at the interior point (x,y); this conforms with the convex-hull construction.

It should be pointed out that the convex hull should be taken with respect to parameters on which the density matrix depends *linearly*, such as x and y in the example of $\rho(x,y)$. Furthermore, in order to obtain the convex hull of a function, one needs to know the *global* structure of the function—in the present case, $E_\psi(x,y)$. We note that numerical algorithms have been developed for constructing convex hulls [20].

As we have discussed, our route to establishing the entanglement of $\rho(x,y)$ involves the analysis of the entanglement of $|\psi(x,y)\rangle$, which we show in Fig. 4. Although it is not obvious, the corresponding surface fails to be convex near the point $(x,y)=(1,0)$, and, therefore, in this region we must suitably convexify in order to obtain the entanglement of $\rho(x,y)$. To illustrate the properties of the entanglement of $|\psi(x,y)\rangle$ we show, in Fig. 1, the entanglement of $|\psi(x,y)\rangle$ along the line $(x,y)=(0,s)$; evidently this is convex. By contrast, along the line $x+2y=1$ there is a region in which the entanglement is not convex, as Fig. 5 shows. The nonconvexity of the entanglement of $|\psi(x,y)\rangle$ complicates the calculation of the entanglement of $\rho(x,y)$, as it necessitates a procedure for constructing the convex hull in the (as it happens, small) nonconvex region. Elsewhere in the xy plane the entanglement of $\rho(x,y)$ is given directly by the entanglement of $|\psi(x,y)\rangle$.

At worst, convexification would have to be undertaken numerically. However, in the present setting it turns out that

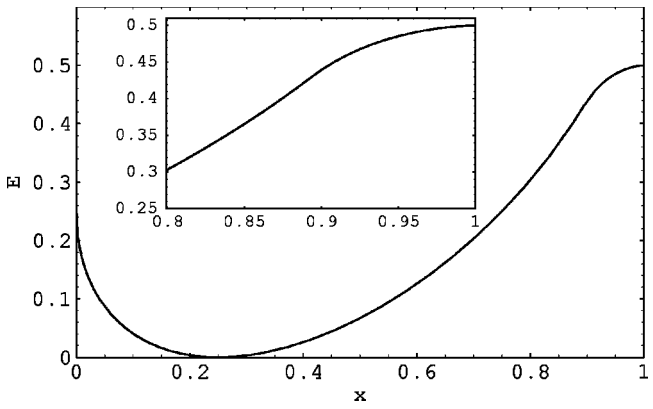

FIG. 5. Entanglement of the pure state $|\psi(x,y=(1-x)/2)\rangle = \sqrt{x}|\mathrm{GHZ}\rangle + \sqrt{(1-x)/2}|W\rangle + \sqrt{(1-x)/2}|\tilde{W}\rangle$ vs x. This shows the entanglement along the diagonal boundary $x+2y=1$. Note the absence of convexity near $x=1$; this region is repeated in the inset.

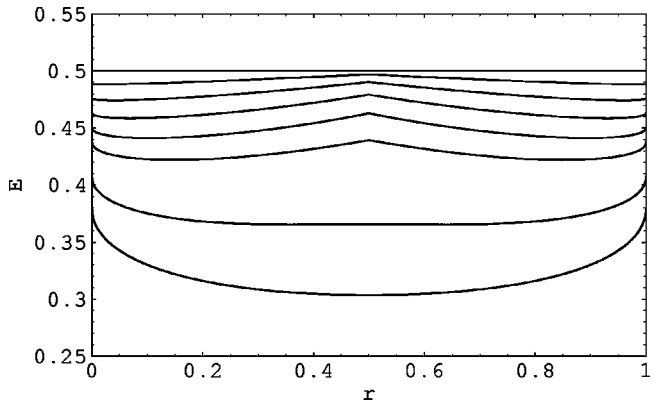

FIG. 7. Entanglement of the pure states $|\psi(x,(1-x)r)\rangle = \sqrt{x}|\mathrm{GHZ}\rangle + \sqrt{(1-x)r}|W\rangle + \sqrt{(1-x)(1-r)}|\tilde{W}\rangle$ vs r for various values of x (from the bottom: 0.8, 0.85, 0.9, 0.92, 0.94, 0.96, 0.98, 1). This reveals the nonconvexity in r for intermediate values of x.

one can determine the convex surface essentially analytically by performing the necessary surgery on surface $z = E_{\psi}(x,y)$. To do this, we make use of the fact that if we parametrize y via $(1-x)r$, i.e., we consider

$$\rho(x,(1-x)r) = x|\mathrm{GHZ}\rangle\langle\mathrm{GHZ}| + (1-x)r|W\rangle\langle W| + (1-x) \times (1-r)|\tilde{W}\rangle\langle\tilde{W}|, \tag{72}$$

where $0 \leqslant r \leqslant 1$ [and similarly for $|\psi(x,y)\rangle$], then, as a function of (x,r), the entanglement will be symmetric with respect to $r=1/2$, as Fig. 6 makes evident. With this parametrization, the nonconvex region of the entanglement of $|\psi\rangle$ can more clearly be identified.

To convexify this surface we adopt the following convenient strategy. First, we reparametrize the coordinates, exchanging y by $(1-x)r$. Now, owing to the linearity, in r at fixed x and vice versa, of the coefficients x, $(1-x)r$, and $(1-x)(1-r)$ in Eq. (72), it is certainly necessary for the entanglement of ρ to be a convex function of r at fixed x and vice versa. Convexity is, however, not necessary in other directions in the (x,r) plane, owing to the nonlinearity of the the coefficients under simultaneous variations of x and r. Put more simply: convexity is not necessary throughout the (x,r) plane because straight lines in the (x,r) plane do not correspond to straight lines in the (x,y) plane (except along lines parallel either to the r or the x axis). Thus, our strategy will be to convexify in a restricted sense: first along lines parallel to the r axis and then along lines parallel to the x axis. Having done this, we shall check to see that no further convexification is necessary.

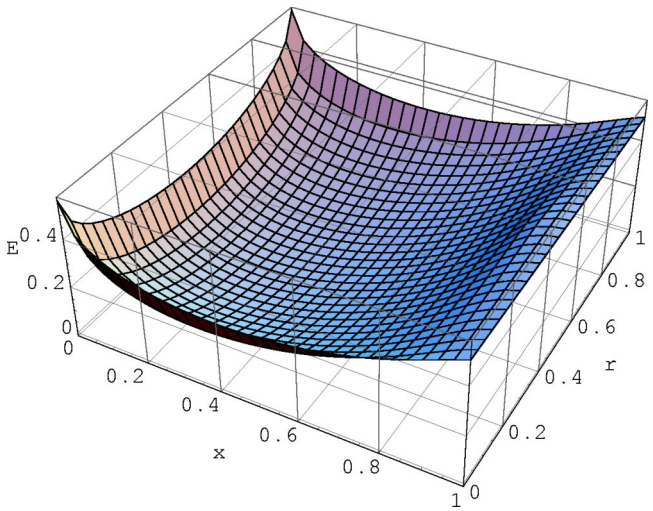

FIG. 6. (Color online) Entanglement of the pure state $|\psi(x,(1-x)r)\rangle = \sqrt{x}|\mathrm{GHZ}\rangle + \sqrt{(1-x)r}|W\rangle + \sqrt{(1-x)(1-r)}|\tilde{W}\rangle$ vs x and r. Note the symmetry of the surface with respect with $r=1/2$.

For each x, we convexify the curve $z = E_{\psi}(x,(1-x)r)$ as a function of r and then generate a new surface by allowing x to vary. More specifically, the nonconvexity in this direction has the form of a symmetric pair of minima located on either side of a cusp, as shown in Fig. 7. Thus, to correct for it, we simply locate the minima and connect them by a straight line.

What remains is to consider the issue of convexity along the x (i.e., at fixed r) direction for the surface just constructed. In this direction, nonconvexity occurs when x is, roughly speaking, greater than 0.8, as Fig. 8 suggests. In contrast with the case of nonconvexity at fixed r, this nonconvexity is due to an inflection point at which the second derivative vanishes. To correct for it, we locate the point $x = x_0$ such that the tangent at $x = x_0$ is equal to that of the line between the point on the curve at x_0 and the end point at $x = 1$, and connect them with a straight line. This furnishes us with a surface convexified with respect to x (at fixed r) and vice versa.

Armed with this surface, we return to the (x,y) parametrization, and ask whether or not it is fully convex (i.e., convex along straight lines connecting *any* pair of points). Equivalently, we ask whether or not any further convexification is required. Although we have not proven it, on the basis of extensive numerical exploration we are confident that the resulting surface is, indeed, convex. The resulting convex entanglement surface for $\rho(x,y)$ is shown in Fig. 9. Figure 10 exemplifies this convexity along the line $2y+x=1$. We

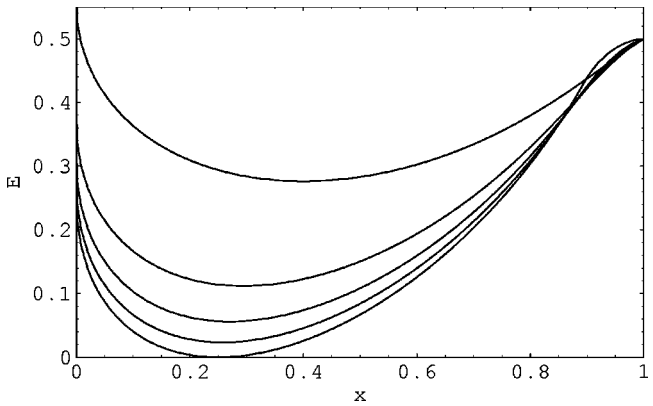

FIG. 8. Entanglement of the pure states $|\psi(x,(1-x)r)\rangle = \sqrt{x}|\mathrm{GHZ}\rangle + \sqrt{(1-x)r}|W\rangle + \sqrt{(1-x)(1-r)}|\widetilde{W}\rangle$ vs x for various values of r (from the top: 0, 0.1, 0.2, 0.3, and 0.5). This reveals the nonconvexity in x in the (approximate) interval $[0.85,1]$.

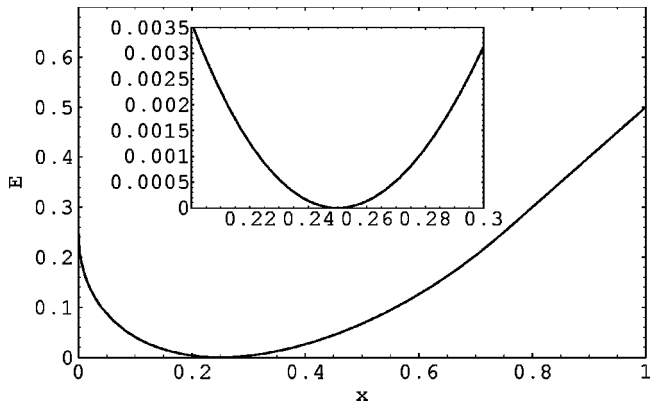

FIG. 10. Entanglement of the mixed state $\rho(x,y=(1-x)/2) = x|\mathrm{GHZ}\rangle\langle\mathrm{GHZ}| + (1-x)/2(|W\rangle\langle W| + |\widetilde{W}\rangle\langle\widetilde{W}|)$ vs x. Inset: enlargement of the region $x \in [0.2,0.3]$. This contains the only point $(x,y)=(1/4,3/8)$, at which $E_\rho(x,y)$ vanishes.

have observed that for the case at hand it is adequate to correct for nonconvexity only in the x direction at fixed r.

C. Comparison with the negativity

This measure of entanglement is defined to be twice the absolute value of the sum of the negative eigenvalues of the partial transpose of the density matrix [7,21]. In the present setting, viz., the family $\rho(x,y)$ of three-qubit states, the partial transpose may equivalently be taken with respect to any one of the three parties, owing to the invariance of $\rho(x,y)$ under all permutations of the parties. Transposing with respect to the third party, one has

$$N(\rho) \equiv -2 \sum_{\lambda_i<0} \lambda_i , \tag{73}$$

where the λ's are the eigenvalues of the matrix ρ^{T_3},

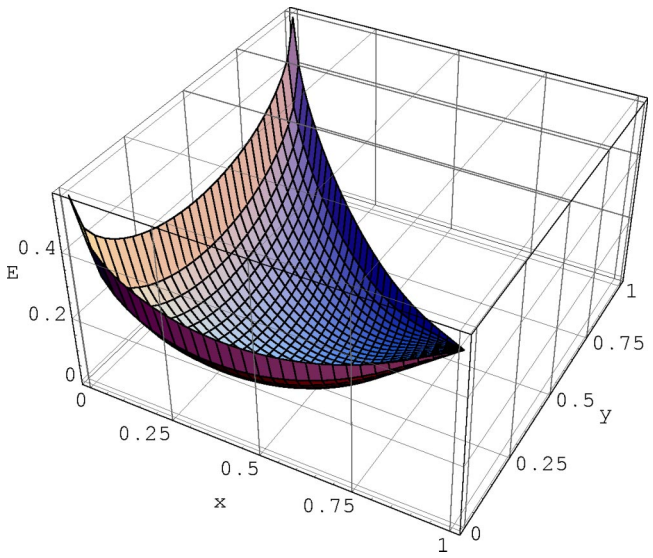

FIG. 9. (Color online) Entanglement of the mixed state $\rho(x,y)$.

It is straightforward to calculate the negativity of $\rho(x,y)$; the results are shown in Fig. 11. Interestingly, for all allowed values of (x,y), the state $\rho(x,y)$ has nonzero negativity, except at $(x,y)=(1/4,3/8)$, at which the calculation of the GME shows that the density matrix is indeed separable. One also sees that $\rho(1/4,3/8)$ is a separable state from the fact that it can be obtained by applying the projection $\mathbf{P}_4$ to the (unnormalized) separable pure state $(|0\rangle+|1\rangle)^{\otimes 3}$. The fact that the only positive-partial-transpose (PPT) state is separable implies that there are no entangled PPT states (i.e., no PPT bound entangled states) within this family of three-qubit mixed states. The negativity surface, Fig. 11, is qualitatively—but not quantitatively—the same as that of GME. By inspecting the negativity and GME surfaces one can see that they present ordering difficulties. This means that one can find pairs of states $\rho(x_1,y_1)$ and $\rho(x_2,y_2)$ that have respective negativities N_1 and N_2 and GMEs E_1 and E_2

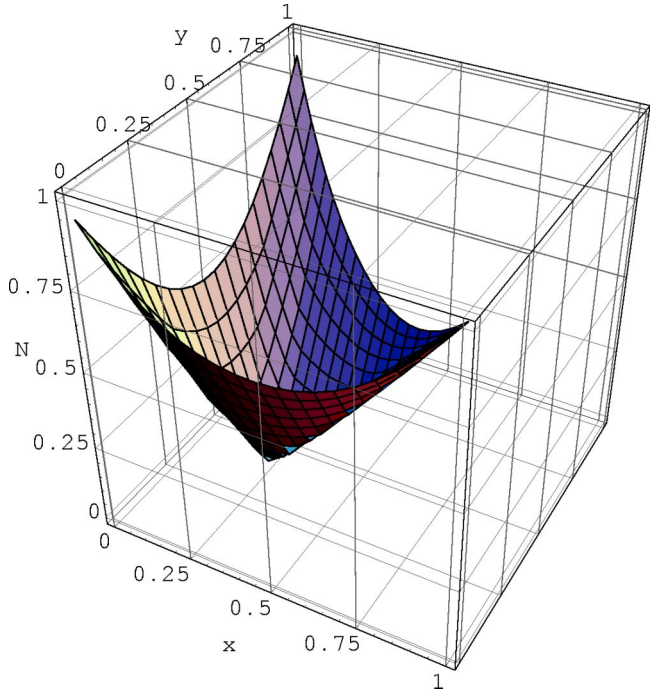

FIG. 11. (Color online) Negativity of the mixed state $\rho(x,y)$.

such that, say, $N_1 < N_2$ but $E_1 > E_2$. Equivalently, the negativity and the GME do not necessarily agree on which of the pair of states is the more entangled. For two-qubit settings, such ordering difficulties do not show up for pure states but can for mixed states [21,22]. On the other hand, for three qubits, such ordering difficulties already show up for pure states, as the following example shows: $N(\mathrm{GHZ}) = 1 > N(W) = 2\sqrt{2}/3$, whereas for the GME the order is reversed. We note, however, that for the relative entropy of entanglement E_R, one has $E_R(\mathrm{GHZ}) = 1 < E_R(W) = \log_2(9/4)$ [23], which for this particular case is in accord with the GME.

VI. CONCLUDING REMARKS

We have considered a rather general, geometrically motivated, measure of entanglement, applicable to pure and mixed quantum states involving arbitrary numbers and structures of parties. In bipartite settings, this approach provides an alternative—and generally inequivalent—measure to the entanglement of formation. For multipartite settings, there is, to date, no explicit generalization of entanglement of formation [23]. However, if such a generalization should emerge, and if it should be based on the convex-hull construction (as it is in the bipartite case), then one may be able to calculate the entanglement of formation for the families of multipartite mixed states considered in the present paper.

As for explicit implementations, the geometric measure of entanglement yields analytic results in several bipartite cases for which the entanglement of formation is already known. These cases include (i) arbitrary two-qubit mixed, (ii) generalized Werner, and (iii) isotropic states. Furthermore, we have obtained the geometric measure of entanglement for certain multipartite mixed states, such as mixtures of symmetric states. In addition, by making use of the geometric measure, we have addressed the entanglement of a rather general family of three-qubit mixed states analytically (up to root finding). This family consists of arbitrary mixtures of GHZ, *W*, and inverted-*W* states. To the best of our knowledge, corresponding results have not, to date, been obtained for other measures of entanglement, such as entanglement of formation and relative entropy of entanglement. We have also obtained corresponding results for the negativity measure of entanglement. Among other things, we have found that there are no PPT bound entangled states within this general family.

A significant issue that we have not discussed is how to use the geometric measure to provide a classification of entanglement of various multipartite entangled states, even in the pure-state setting. For example, given a tripartite state, is all the entanglement associated with pairs of parts or is some attributable only to the system as a whole? More generally, one can envisage all possible partitionings of the parties, and for each compute the geometric measure of entanglement. This would provide a hierarchical characterization of the entanglement of states, more refined than the global characterization discussed here. Another extension would involve augmenting the set of separable pure states with certain classes of entangled pure states, such as biseparable entangled, *W*-type, and GHZ-type states [24].

Although there is no generally valid analytic procedure for computing the entanglement eigenvalue $\Lambda_{\max}$, one can give—and indeed we have given—analytical results for several elementary cases. Harder examples require computation, but often this is (by today's computational standards) trivial. We note that in order to find $\Lambda_{\max}$ for the state $|\psi\rangle$ it is not necessary to solve the nonlinear eigenproblem (5); one can instead appropriately parametrize the family of separable states $|\phi\rangle$ and then directly maximize their overlap with the entangled state $|\psi\rangle$, i.e., $\Lambda_{\max} = \max_{\phi} \| \langle \phi | \psi \rangle \|$. Besides, we mention that there exist numerical techniques for determining E_{F} (see, e.g., Ref. [25]). We believe that numerical techniques for solving the geometric measure of entanglement for general multipartite mixed states can readily be developed.

The motivation for constructing the measure discussed in the present paper is that we wish to address the degree of entanglement from a geometric viewpoint, regardless of the number of parties. Although the construction is purely geometric, we have related this measure to entanglement witnesses, which can in principle be measured locally [15]. Moreover, the geometric measure of entanglement is related to the probability of preparing a single copy of a two-qubit mixed state from a certain pure state [18]. Yet it is still desirable to see whether, in general, this measure can be associated with any physical process in quantum information, as are the entanglement of formation and distillation.

There are further issues that remain to be explored, such as additivity and ordering. The present form of entanglement for pure states, $E_{\sin^2} \equiv 1 - \Lambda^2$, is not additive. However, one can consider a related form, $E_{\ln} \equiv -\ln \Lambda^2$, which, e.g., is additive for $|\psi\rangle_{AB} \otimes |\psi\rangle_{CD}$, i.e.,

$$E_{\ln}(|\psi_1\rangle_{AB} \otimes |\psi_2\rangle_{CD}) = E_{\ln}(|\psi_1\rangle_{AB}) + E_{\ln}(|\psi_2\rangle_{CD}). \tag{74}$$

This suggests that it is more appropriate to use this logarithmic form of entanglement to discuss additivity issues. However, it remains to check whether it is an entanglement monotone when extended to mixed states by convex hull.

As regards the ordering issue, we first mention a result of bipartite entanglement measures, due to Virmani and Plenio [22], which states that any two measures with continuity that give the same value as the entanglement of formation for *pure* states are ''either identical or induce different orderings in general.'' This result points out that different entanglement measures will inevitably induce different orderings if they are inequivalent. This result might still hold for multipartite settings, despite their discussion being based on the existence of entanglement of formation and distillation, which have not been generalized to multipartite settings. Although the geometric measure gives the same ordering as the entanglement of formation for two-qubit mixed states [see Eq. (45)], we believe that the geometric measure will, in general, give a different ordering. However, it is not our intention to discuss the ordering difficulty in the present paper. Nevertheless, it is interesting to point out that for bipartite systems, even though the relative entropy of entanglement coincides with

entanglement of formation for pure states, they can give different orderings for mixed states, as pointed out by Verstraete *et al.* [22].

We conclude by remarking that the measure discussed in the present paper is not included among the infinitely many different measures proposed by Vedral *et al.* [26]. These measures are based on the minimal distance between the entangled mixed state and the set of separable *mixed* states. By contrast, the measure considered here is based upon the minimal distance between the entangled pure state and the set of separable pure states, and it is extended to mixed states by a convex-hull construction.

ACKNOWLEDGMENTS

We thank J. Altepeter, H. Barnum, D. Bruß, W. Dür, H. Edelsbrunner, J. Eisert, A. Ekert, M. Ericsson, O. Gühne, L.-C. Kwek, P. Kwiat, D. Leung, C. Macchiavello, S. Mukhopadhyay, Y. Omar, M. Randeria, F. Verstraete, G. Vidal, and especially W. J. Munro for discussions. P.M.G. acknowledges the hospitality of the University of Colorado-Boulder and the Aspen Center for Physics. This work was supported by NSF Grant No. EIA01-21568 and U.S. DOE Grant No. DEFG02-91ER45439. T.C.W. also acknowledges the hospitality of the Benasque Center for Science, where part of the revision was done.

APPENDIX: THE VOLLBRECHT-WERNER TECHNIQUE

In this appendix, we now briefly review a technique developed by Vollbrecht and Werner [4] for computing the entanglement of formation for the generalized Werner states; this turns out to be applicable to the computation of the sought quantity $E_{\sin^2}$. We start by fixing some notation. Let (a) K be a compact convex set (e.g., a set of states that includes both pure and mixed ones); (b) M be a convex subset of K (e.g., set of pure states); (c) $E:M\to R\cup\{+\infty\}$ be a function that maps elements of M to the real numbers (e.g., $E=E_{\sin^2}$); and (d) G be a compact group of symmetries, acting on K (e.g., the group $U\otimes U^{\dagger}$) as $\alpha_g:K\to K$ (where α_g is the representation of the element $g\in G$) that preserve convex combinations.

We assume that $\alpha_g M\subset M$ (e.g., pure states are mapped into pure states), and that $E(\alpha_g m)=E(m)$ for all $m\in M$ and $g\in G$ (e.g., that the entanglement of a pure state is preserved under α_g). We denote by $\mathbf{P}$ the invariant projection operator defined via

$$\mathbf{P}k=\int dg\ \alpha_g(k), \tag{A1}$$

where $k\in K$. Examples of $\mathbf{P}$ are the operations $\mathbf{P}_1$ and $\mathbf{P}_2$ in the main text. Vollbrecht and Werner also defined the following real-valued function ϵ on the invariant subset $\mathbf{P}K$:

$$\epsilon(x)=\inf\{E(m)\,|\,m\in M,\mathbf{P}m=x\}. \tag{A2}$$

They then showed that, for $x\in\mathbf{P}K$,

$$\mathcal{C}_{\rm conv}E(x)=\mathcal{C}_{\rm conv}\epsilon(x), \tag{A3}$$

and provided the following recipe for computing the function $\mathcal{C}_{\rm conv}E$ for G-invariant states: (1) For every invariant state ρ (i.e., obeying $\rho=\mathbf{P}\rho$), find the set M_ρ of pure states σ such that $\mathbf{P}\sigma=\rho$; (2) compute $\epsilon(\rho)\equiv\inf\{E(\sigma)\,|\,\sigma\in M_\rho\}$; (3) then $\mathcal{C}_{\rm conv}E$ is the convex hull of this function ϵ.

[1] See, e.g., M. Nielsen and I. Chuang, *Quantum Computation and Quantum Information* (Cambridge University Press, Cambridge, 2000).
[2] For a review, see M. Horodecki, Quantum Inf. Comput. **1**, 3 (2001), and references therein.
[3] W.K. Wootters, Phys. Rev. Lett. **80**, 2245 (1998).
[4] K.G.H. Vollbrecht and R.F. Werner, Phys. Rev. A **64**, 062307 (2001).
[5] B.M. Terhal and K.G.H. Vollbrecht, Phys. Rev. Lett. **85**, 2625 (2000).
[6] V. Vedral and M.B. Plenio, Phys. Rev. A **57**, 1619 (1998).
[7] K. Życzkowski, P. Horodecki, A. Sanpera, and M. Lewenstein, Phys. Rev. A **58**, 883 (1998); G. Vidal and R.F. Werner, *ibid.* **65**, 032314 (2002).
[8] J. Eisert and H.J. Briegel, Phys. Rev. A **64**, 022306 (2001).
[9] A. Shimony, Ann. N.Y. Acad. Sci. **755**, 675 (1995).
[10] H. Barnum and N. Linden, J. Phys. A: Math. Gen. **34**, 6787 (2001).
[11] We thank M. Randeria for a discussion on this point.
[12] J.K. Stockton, J.M. Geremia, A.C. Doherty, and H. Mabuchi, Phys. Rev. A **67**, 022112 (2003).
[13] S. Bravyi, Phys. Rev. A **67**, 012313 (2003).
[14] M. Horodecki, P. Horodecki, and R. Horddecki, Phys. Lett. A **223**, 1 (1996).
[15] O. Gühne, P. Hyllus, D. Bruß, A. Ekert, M. Lewenstein, C. Macchiavello, and A. Sanpera, Phys. Rev. A **66**, 062305 (2002).
[16] M. Horodecki, P. Horodecki, and R. Horodecki, Phys. Rev. Lett. **84**, 2014 (2000).
[17] G. Vidal, J. Mod. Opt. **47**, 355 (2000).
[18] G. Vidal, Phys. Rev. A **62**, 062315 (2000).
[19] M. Horodecki and P. Horodecki, Phys. Rev. A **59**, 4206 (1999).
[20] See e.g., C.B. Barber, D.P. Dobkin, and H.T. Huhdanpaa, ACM Trans. Math. Softw. **22**, 469 (1996).
[21] T.C. Wei, K. Nemoto, P.M. Goldbart, P.G. Kwiat, W.J. Munro, and F. Verstraete, Phys. Rev. A **67**, 022110 (2003).
[22] This ordering difficulty has been discussed in the settings of two qubits in many places, e.g., J. Eisert and M.B. Plenio, J. Mod. Opt. **46**, 145 (1999); K. Życzkowski, Phys. Rev. A **60**, 3496 (1999); S. Virmani and M.B. Plenio, Phys. Lett. A **268**, 31 (2000); F. Verstraete *et al.*, J. Phys. A **34**, 10 327 (2001), as well as in Ref. [21].
[23] M.B. Plenio and V. Vedral, J. Phys. A **34**, 6997 (2001).
[24] A. Acín, D. Bruß, M. Lewenstein, and A. Sanpera, Phys. Rev. Lett. **87**, 040401 (2001).
[25] K. Życzkowski, Phys. Rev. A **60**, 3496 (1999).
[26] V. Vedral, M.B. Plenio, M.A. Rippin, and P.L. Knight, Phys. Rev. Lett. **78**, 2275 (1997).